NASA/TM-20230009958

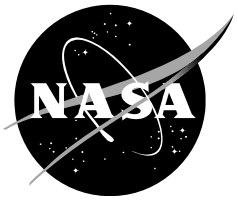

New Retropropulsion Concept with NTAC Power for Mars Entry

Sang H. Choi
NASA Langley Research Center, Hampton, VA

Holt R. Moses
Old Dominion University, Norfolk, VA

Robert W. Moses
Tamer Space, LLC., Poquoson, VA

Ronald Merski
NASA Langley Research Center, Hampton, VA

National Aeronautics and
Space Administration

NASA Langley Research Center
Hampton, VA

August 2023

NASA STI Program ... in Profile

Since its founding, NASA has been dedicated to the advancement of aeronautics and space science. The NASA scientific and technical information (STI) program plays a key part in helping NASA maintain this important role.

The NASA STI program operates under the auspices of the Agency Chief Information Officer. It collects, organizes, provides for archiving, and disseminates NASA's STI. The NASA STI program provides access to the NTRS Registered and its public interface, the NASA Technical Reports Server, thus providing one of the largest collections of aeronautical and space science STI in the world. Results are published in both non-NASA channels and by NASA in the NASA STI Report Series, which includes the following report types:

TECHNICAL PUBLICATION. Reports of completed research or a major significant phase of research that present the results of NASA Programs and include extensive data or theoretical analysis. Includes compilations of significant scientific and technical data and information deemed to be of continuing reference value. NASA counterpart of peer-reviewed formal professional papers but has less stringent limitations on manuscript length and extent of graphic presentations.

TECHNICAL MEMORANDUM. Scientific and technical findings that are preliminary or of specialized interest, e.g., quick release reports, working papers, and bibliographies that contain minimal annotation. Does not contain extensive analysis.

CONTRACTOR REPORT. Scientific and technical findings by NASA-sponsored contractors and grantees.

CONFERENCE PUBLICATION. Collected papers from scientific and technical conferences, symposia, seminars, or other meetings sponsored or co-sponsored by NASA.

SPECIAL PUBLICATION. Scientific, technical, or historical information from NASA programs, projects, and missions, often concerned with subjects having substantial public interest.

TECHNICAL TRANSLATION. English-language translations of foreign scientific and technical material pertinent to NASA's mission.

Specialized services also include organizing and publishing research results, distributing specialized research announcements and feeds, providing information desk and personal search support, and enabling data exchange services.

For more information about the NASA STI program, see the following:

Access the NASA STI program home page at http://www.sti.nasa.gov

E-mail your question to help@sti.nasa.gov

Phone the NASA STI Information Desk at 757-864-9658

Write to:
NASA STI Information Desk
Mail Stop 148
NASA Langley Research Center
Hampton, VA 23681-2199

NASA/TM-20230009958

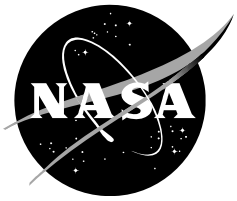

New Retropropulsion Concept with NTAC Power for Mars Entry

Sang H. Choi
NASA Langley Research Center, Hampton, VA

Holt R. Moses
Old Dominion University, Norfolk, VA

Robert W. Moses
Tamer Space, LLC., Poquoson, VA

Ronald Merski
NASA Langley Research Center, Hampton, VA

National Aeronautics and
Space Administration

NASA Langley Research Center
Hampton, VA

August 2023

Table of Contents

Abstract 5

Nomenclatures 5

I. Introduction 6
II. Design and Variables 9

II-1. Entry Model Design 9

II-2. Atmospheric and Design Variables 11

III. Rough Estimations and Results 14

III-1. Bases for Calculations 14

III-2. Performance Analysis of new retropropulsion system Conclusion 18

IV. Conclusion 22

References 23

Abstract

Since the initial deployments of probes, orbiters, and rovers on Mars, there have been many ideas and concepts on how to perform an entry, descent, and landing (EDL) process efficiently and safely through the Martian atmosphere to place payloads onto the surface of Mars. Among the missions sent to perform EDL on Mars, only roughly sixty percent of the missions have been successful. The 5 minutes to 20 minutes of communication gap due to long-range telecommunications to Earth, described as seven minutes of terror, add to the complexity of EDL missions to Mars. As the payloads have become larger, the method of EDL has become more complex. To place an automobile-size science rover on the Martian surface requires the use of retrorockets mounted on a Sky Crane during the final subsonic stage of EDL. Larger payloads will require more propellant and more and/or larger retropropulsion engines during the earlier supersonic stage of EDL. The Sky Crane concept may not be scalable for these larger payloads and during supersonic flight; hence, new approaches are sought. A new power technology invented at NASA called Nuclear Thermionic Avalanche Cell (NTAC) may offer an additional solution. Powered by NTAC, the newly invented retropropulsion concept would ingest carbon dioxide gas, heat it up and blast it out as a new feature of the EDL process. NTAC would be reusable as a primary power source for payloads such as excavators, three-dimensional (3D) printers, or mobile equipment for mining, construction, and additive manufacturing tasks. Since NTAC would need to be landed with its host payload or as a standalone power package, assessing its ability to assist in its own EDL seems reasonable. The purpose of this Technical Memorandum (TM) is to examine the performance of NTAC in the context of EDL at Mars for motivating studies for integrating NTAC into future Mars mission architectures.

Nomenclatures

A_{inlet} -	Inlet Area of ingested port, m^2
h -	Altitude, m
I_{SP} -	Specific impulse, sec
$I_{SP\Delta p}$ -	Specific impulse gain by pressure difference, sec
$I_{SP\text{-}Total}$ -	= I_{SP} + $I_{SP\Delta p}$
$\dot{m}$ -	Flowrate of ingested gas, kg/sec
M -	Molecular weight
p -	Pressure, kPa
p_{BS} -	Pressure at behind the shock, kPa
p_{enter} -	Pressure of altitude-dependent gas, kPa
p_{exit} -	Pressure at nozzle exit, kPa
p_{inlet} -	Pressure of ingested gas, kPa

$p_{Heating}$ - Pressure of heated gas, kPa

$P_{Heating}$ - Power required for heating the ingested gas, kW

P_{MW} - Power in megawatt, MW

R - Gas constant, 8.314 $J \cdot K^{-1} \cdot mol^{-1}$

T - Temperature, K

T_{mixed} - Temperature of mixed gas of shock-layer and free stream, K

$T_{ambient}$ - Temperature of free-stream or ambient gas, K

T_{max} - Maximum allowable temperature, = 2800 K

$V_{vehicle}$ - Velocity of entry vehicle, m/sec

$V_{Heating}$ - Gas velocity through heated channel for retropropulsion, m/sec

$V_{\Delta p}$ - Velocity gain by pressure difference, m/sec

ρ - Density, kg/m^3

ρ_∞ or ρ_{FS} - Free-stream density, kg/m^3

ρ_{SL} - Shock-layer density, kg/m^3

ρ_{Inlet} - Density of ingested gas, kg/m^3

$\gamma \ (= {}^{c_p}/_{c_v})$ - Specific heat ratio = 1.28 for CO_2

I. Introduction

The successful landing of the *Viking 1* and *Viking 2* landers on Mars on July 20, 1976 and September 3, 1976, respectively, allowed access to the Martian surface to increase our understanding of the challenges and opportunities for science and human missions there. Since then, the progress for Mars probe exploration has gradually increased to include large science rovers that require new methods for Entry, Descent, and Landing (EDL). The EDL process for Mars missions greatly imposes a technical dilemma due largely to the 5 minutes to 20 minutes communication gap between the Earth and Mars. Only about 60% of those missions were successful for a number of reasons [1]. This is because spacecraft with payload descending into the atmosphere requires fast communications for command, control, and monitoring to steer the spacecraft for safe landing on Mars. However, a communication signal takes about 11 minutes to reach Earth once sent from Mars. This reality requires that the Mars EDL process act independently and autonomously.

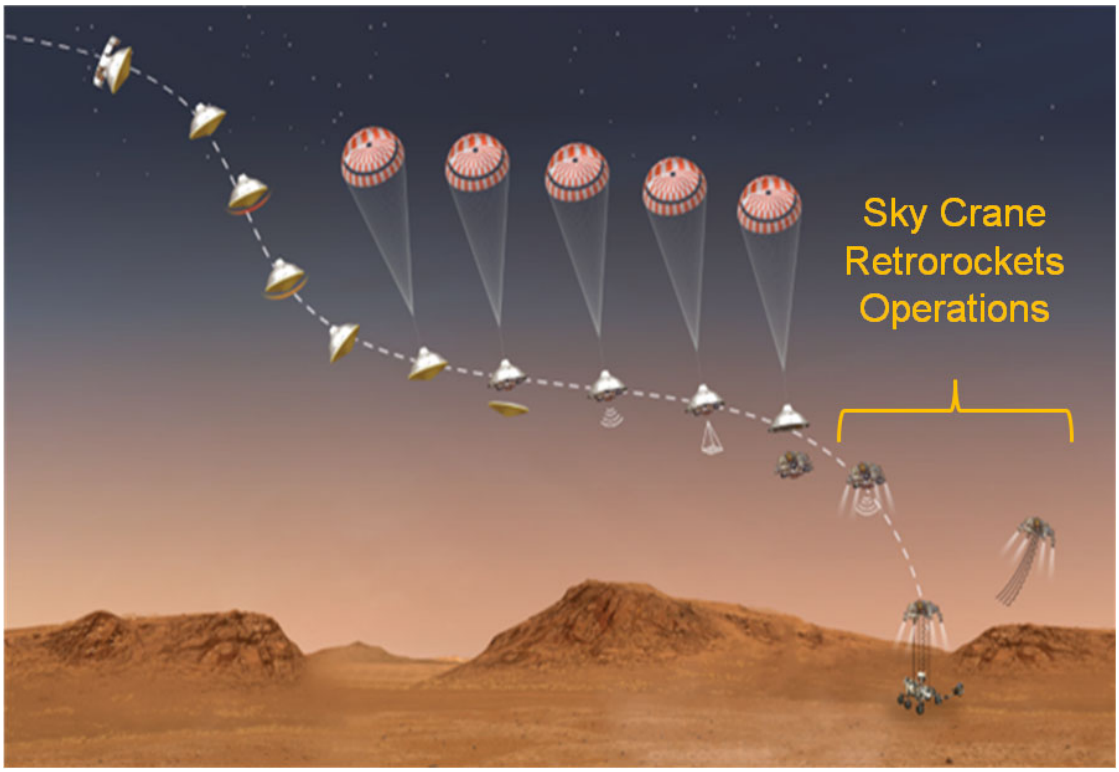

Figure 1. Perseverance Rover's Entry, Descent, and Landing Profile. [6]

There had been many different EDL methods used for Mars landing [2]. The conventional method of using aerodynamic drag, parachutes, and retro-rocket propulsion to slow-down within the entry flight corridor has been very effective but required carrying a substantial amount of propellant. The current Mars EDL procedure has been used for direct entries from Earth through the atmosphere for placing a lander on the Martian surface [3-5]. Illustrated in Figure 1 are the events that occurred in the final minutes of the nearly seven-month journey that the NASA *Perseverance* rover took to Mars [6]. This Mars EDL process begins with an aerodynamic drag phase, followed by the supersonic parachute deployment for slowing-down further at the mid stage, and finally the blast of retrorockets mounted on a Sky Crane to perform the final stage of touch-down.

As the Mars Program transitions to include astronaut missions involving habitats and crewed rovers, the EDL process will likely require even larger entry vehicles with more powerful retropropulsion capabilities and more propellant mass to be brought from Earth. Furthermore, the retropropulsion will need to operate during supersonic conditions higher in the atmosphere in order for the entry vehicle to reach subsonic flight in time to land safely [7]. It is not clear whether the sky crane concept will scale up as the payload size and mass increase by an order of magnitude. Hence, as the payloads continue to become larger, new EDL approaches are sought.

A new power device invented at NASA called Nuclear Thermionic Avalanche Cell (NTAC) [8] may offer a means to land larger payloads on Mars, as well as to reduce the amount of propellant brought from Earth in two ways: 1) reduce by at least 10% ~ 20% level by heating the propellant gas (brought from Earth) for both acceleration period after launching from the Moon or Mars and

deceleration period before landing on the moon and Mars; 2) reheat atmospheric gas collected during descent at Mars as retropropulsion during the initial stage of the Mars entry process, as illustrated in Figure 2. A brief study of the latter was conducted to show the benefit of this new concept using the Mars atmosphere for retropropulsion. The results of that study are presented herein.

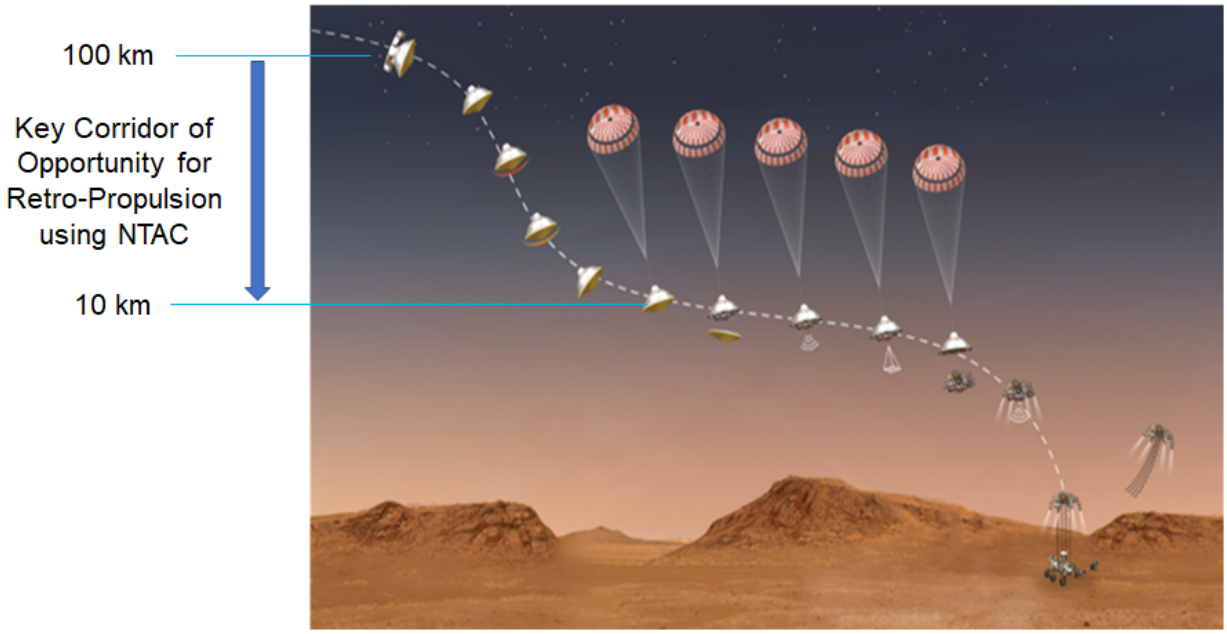

Figure 2. Portion of EDL Profile for Assessing NTAC Performance.

The Concept of Operations is described as follows: The entry vehicle enters the Martian atmosphere. As the entry vehicle reaches an altitude of 100 km, a shock layer forms around the leading edge (called forebody) of the entry vehicle. The temperatures and pressures between the forebody and the shock layer are higher than ambient free-stream conditions. This new retropropulsion system has an ingestion port at the axial symmetry centerline of the forebody. This port ingests carbon dioxide (CO_2) gas from the Martian atmosphere causing the shock layer to collapse into the port while also allowing ingestion of free-stream gas that mixes with the ingested portion of shock layer, as illustrated in Figure 3. In this case, since the ingested gas is the mixture of free-stream gas and a portion of the collapsed shock layer, the overall temperature of ingested mixture gas will be higher than that of free-stream by as much as the injected contribution of high temperature gas of shock layer. In this study, the ingested gas consists of a majority portion up to 90% level of the free-stream and the rest by the shock layer formed around the edge of port [9]. This ingested gas runs through the curved channels formed after splitting the ingestion port into several branch channels. While the mixture gas passes through the split curved channels where thermal energy is added into the flow-field by the NTAC power system, it is considered that the mixture gas is heated to no more than a designated temperature, such as 2800 K. The maximum allowable temperature is determined by the tolerance of materials used for the curved channels and heater. The expanded ejection of heated gas through the nozzles of

curved channels generates retropropulsion intended to slow down the vehicle as it descends through the atmosphere. At 10 km, the parachute will be deployed to further decelerate the descending entry vehicle.

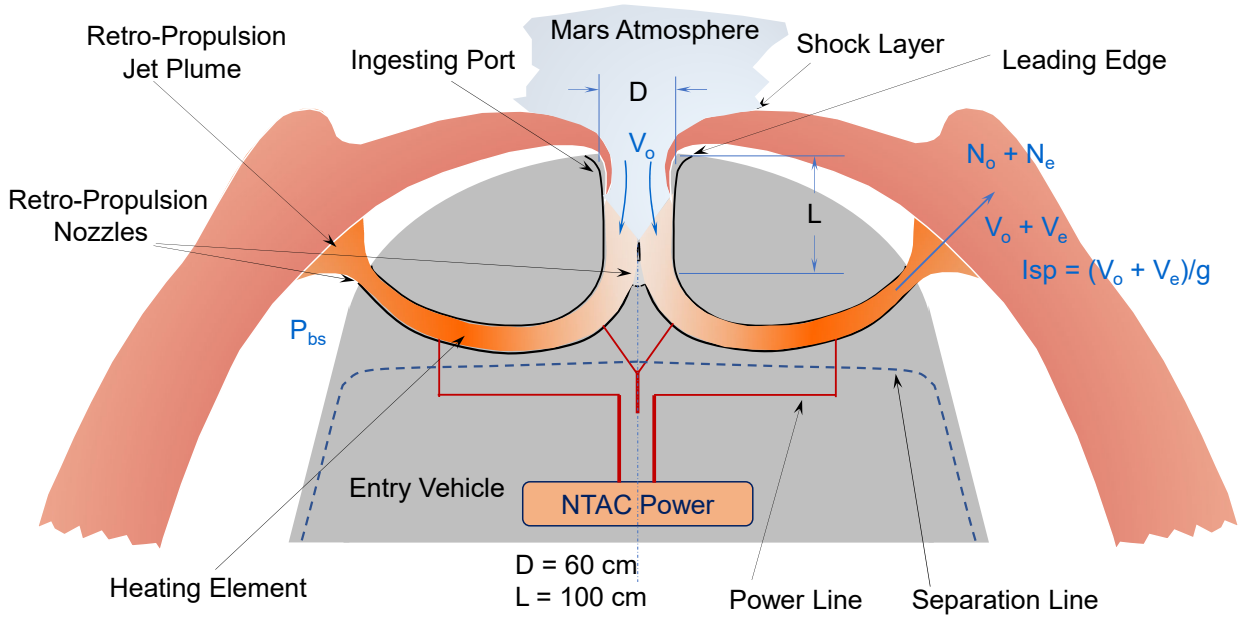

Figure 3. Invented Concept of NTAC powered Mars entry model with Ingestion Port.

II. Design and Variables

II-1. Entry Model Design

The new concept is to use the resources such as the gases in the Mars atmosphere to create retropropulsion. To slow down a large Mars entry vehicle, a new retropropulsion approach that uses NTAC is considered in this study. The new retropropulsion concept, illustrated in Figure 3, outfits a vehicle with an ingestion port integrated at the central stagnation point of the entry leading edge of the vehicle where the shock layer forms and collapses into the ingestion port. The ingested gas is heated up to 2800 K using heating coils or heating elements located within the split curved channels that blasts out the heated gas at 2800 K through the nozzles of each channel to generate retropropulsion thrust. This process continues until the speed of the lander decreases to allow for parachute deployment. In Figure 3 the configuration and major components of the retropropulsion system are shown. The top view of the new retropropulsion system is shown in Figure 4.

For the nose configuration shown in Figure 3, the shock layer developed around the edge of the port drops off and is entrained and mixed with the free-stream gas that flows through the port. The shock layer is a high temperature compressed gas. Once the cold free-stream gas is mixed with the portion of the shock layer formed around the opening edge of the port, the temperature

of the mixed gas is raised to a level determined by the mixture ratio. For the purpose of this study, the shock layer formed around the edge of the port constitutes about 10% of the total flow through the port. Therefore, the density and temperature of the gas mixture were estimated using roughly a 9 to 1 ratio between the free-stream and shock layer [9] to determine the power requirement for additional heating of mixed gas up to the ultimately allowable temperature, 2800 K. Finally, the heated gas mixture is directed and expanded through the retropropulsion channels that ejects the 2800 K gas through nozzles to produce retropropulsion. As stated previously, NTAC is a simple and compact power system with a very high specific power (> 1 kW/kg) [8] that is used to heat the mixture gas to a desirable temperature.

The heating coils or elements located within the channels are powered by NTAC. The heating elements can be, for example, made from porous refractory metal structure that can be inductively heated. To clarify, the ingested CO_2 gas that passes through the porous metal structure is heated to a desired level for retropropulsion.

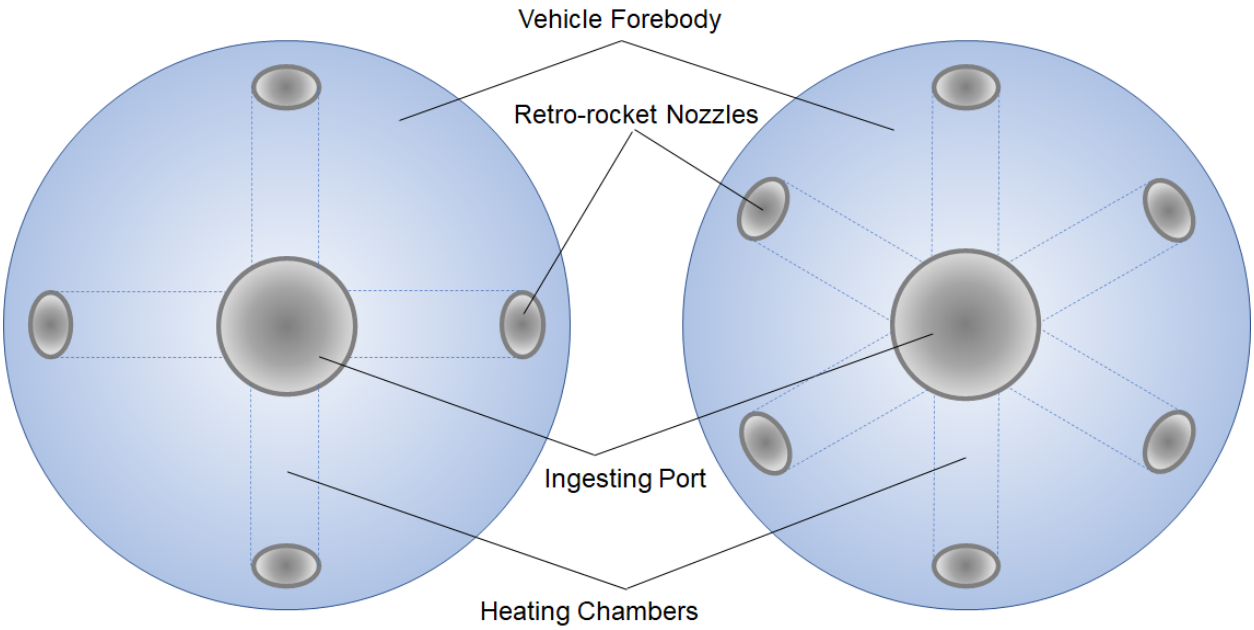

Figure 4. Top view of invented concept of NTAC powered Mars entry model with an ingestion port and 4 (left) or 6 (right) retropropulsion nozzles.

The envisioned configuration of Mars entry model with an ingesting port at the nose of the forebody and 4 or 6 retropropulsion thrust nozzles placed near the trailing edge of the forebody is shown in Figure 4. Studies showed that placement of the retropropulsion nozzles near the trailing edge of the forebody offers the best spacecraft stability performance during supersonic flight conditions [7]. The number of retro-propulsion thrust nozzles can be selected by these operational criteria. The thrust from each nozzle can be individually controlled by the active distribution of the flowrate of CO_2 propellant that comes through the ingesting port. The thrust control of each nozzle can be performed by the heating rate of propellant through power

modulation on each heating element. Such manners of control capabilities can allow a high degree of maneuverability for the entry vehicles during operations of this retropropulsion concept.

In short, the high degree of maneuverability during Mars entry flight can be achievable by:

- Multi-channel thrust nozzles,
- Flowrate distribution control of the CO_2 propellant that is ingested through the port, or
- Heating rate control on each CO_2 propellant channel by power modulation.

II-2. Atmospheric and Design Variables

A vertical structure of the Martian atmosphere overlaid with temperature was constructed by using the data from the entry probes of Mars landers [10-12], shown in Figure 5. The range of retropropulsion operation considered for this analysis is from 100 km to 10 km, annotated in Figure 5. The retropropulsion operation stops at an altitude of 10 km prior to parachute deployment.

The operation of this new concept retropropulsion can be feasibly exercised at or around 100 km because that is where the density of the gas becomes a meaningful level for compressed flow

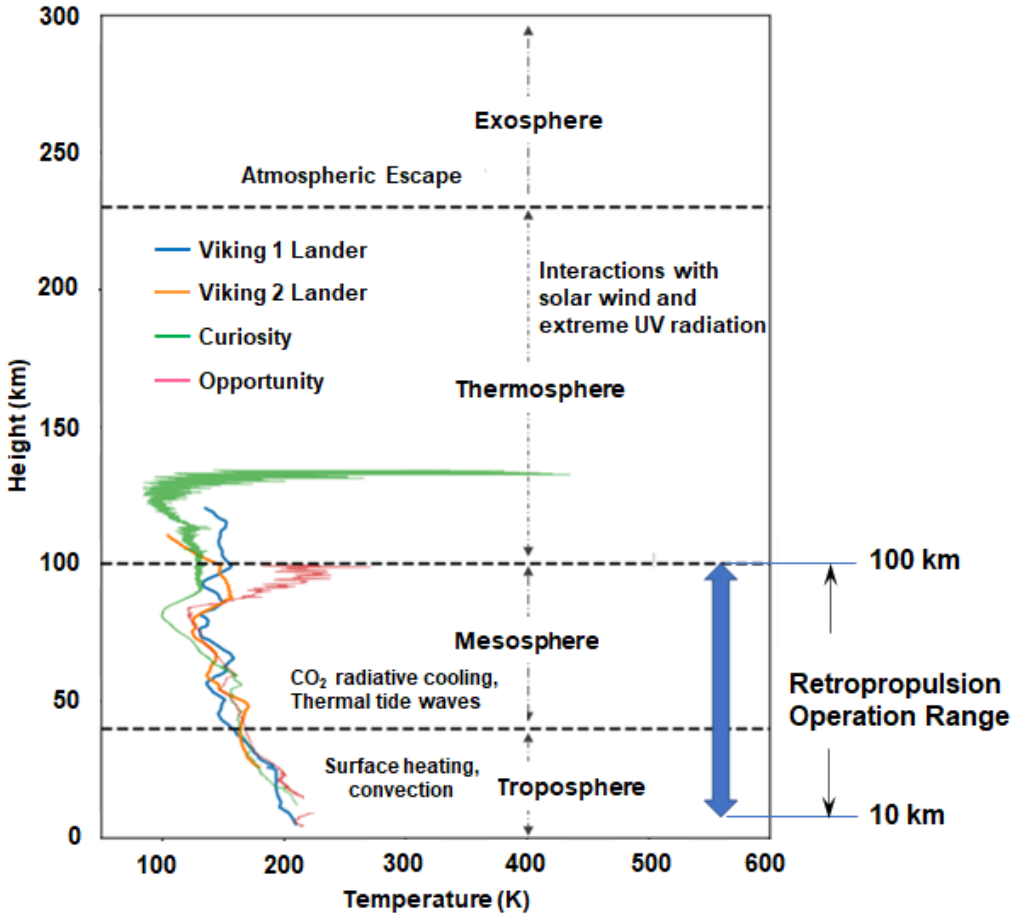

Figure 5. Martian atmospheric structure [9-11] and range of entry process is set from 100 km to 10 km.

over around the forebody of an entry vehicle. The Martian atmosphere is primarily CO_2

(comprising 96%), as well as nitrogen (N_2), oxygen (O_2), carbon monoxide (CO), and atomic oxygen (O). At the altitude of 100 km, the number density of constituent gases is approximately 10^{12} per cm^3 which is equivalent to approximately 4 x 10^{-7} atm [13]. The pressure increases as altitude decreases. When entering the Martian atmosphere, a shock layer forms around the forebody of the entry vehicle. During these hypersonic speeds, the shock layer compresses the atmosphere increasing the atmospheric density, the collision frequency of air molecules, and the temperature of the shock layer, causing the flow to reach an ionized state.

As a reminder, the envisioned integration of the new NTAC-augmented retropropulsion with the entry vehicle, illustrated in Figure 3 and Figure 4, allows the collapse of the shock layer into the opening of ingestion port. The portion of this shock layer formed around the edge of the port opening can not only be sucked into the inside of the port, but also mixed with the free-stream flowing through the central portion of the port. The purpose of NTAC is to elevate the temperature of the atmospheric mixture for use as retropropulsion thrust.

To estimate the thrust and specific impulse of this new retropropulsion system, several important parameters must be given or estimated to describe the densities of gas in the free-stream and the shock layer, the flowrate through the channels, the shock temperature, the temperature of mixed gas, and the pressures. To find an accurate temperature of the shock layer, data from pervious Mars missions were reviewed. As studied by Drake, J.R. et al. [14], the temperature profiles vs. altitude of three different Mars missions were plotted to show temperature data points of the shock layer along their entry passages. The temperature data used in this study comes from the Mars Exploration Rover (MER) *Opportunity* [14].

The ambient temperature, pressure, and density of the Martian atmosphere along with the altitude are tabulated in Table 1. These Mars atmospheric parameters tabulated in Table 1 were calculated using the mathematical model from NASA Glenn Research Center [15]. In this study, the retropropulsion flight envelope selected for the entry and descent level is from 100 km down to 10 km where the supersonic parachute is deployed for further deceleration of the entry vehicle, as depicted in Figure 2.

An important variable to note for ingesting atmospheric gas is the ambient density at the opening port where the shock layer collapses. An example of shock layer on the leading front of entry vehicle is illustrated as a grid-mesh domain [9]. It shows what happens with a leading-edge including shock and boundary layer clustering. The density profile of the shock layer was identified by the ratio of the free-stream density, ρ_∞. The shock layer density, ρ, within the boundary layer drastically increased while the enthalpy of flow medium is kept low [9]. Based on the study done by Leibowitz, M.G. and Austin, J.M. [9], the shock layer density ratio is approximately ten times greater than the density of the free-stream, ρ_∞.

Table 1. Mars Upper Atmosphere Profiles for Temperature, Pressure, and Density [15].

For $h > 7000$ m

$T = -23.4 - 0.00222h$

$p = 0.699\, e^{-0.00009h}$

For $h < 7000$ m

$T = -31 - 0.000998h$

$p = 0.699\, e^{-0.00009h}$

$\rho = p/(0.1921 \cdot (T + 273.2))$

where

ρ = density (kg/m^3) p = pressure (kPa)

T = temperature (C) h = altitude (m)

Altitude, km	Ambient Temperature, K	Pressure, kPa	Density, kg/m^3
100	27.75	0.00008625	0.0000162
80	72.15	0.00052186	0.0000376
60	116.55	0.00315710	0.0001411
50	138.75	0.00776521	0.0002914
40	160.95	0.01909933	0.0006179
30	183.15	0.04697674	0.0013356
20	205.35	0.11554406	0.0029298
10	227.55	0.28419219	0.0065028

Pezzella, G. and Viviani, A. [17] estimated the static pressure of the shock layer around the forebody of the Mars entry vehicle. The static pressure of the shock layer is higher along the forebody of the entry vehicle. In Figure 6, the ingestion port shown in Figure 3 is overlaid on the static pressure profile to illustrate the envisioned modification to the shock layer caused by the flow through the new retropropulsion concept. Shown in Figure 6 is the ingesting port located at the middle of the entry vehicle and the retro-rocket nozzles located downstream of the shock layer. The two thick red color arrows indicate the static pressures at the stagnation point and the downstream of shock layer, respectively. The mixture of free-stream and shock layer gases is ingested and further mixed through the passage as it is reheated by NTAC in the curved heating chambers, as shown in Figure 3. The ingesting port is split into several heating chambers as shown in Figure 4. The number of heating chambers can be determined for the most effective retropropulsion. In any case, the density and temperature of the incoming gas mixture were estimated using roughly a 9 to 1 ratio between the free-stream and shock layer [9] to determine the power requirement to heat the gas mixture up to the ultimate allowable temperature, 2800 K. This ultimate allowable temperature, 2800 K, is selected with the maximum allowable temperature of the materials of the heating element and chamber in mind. If the portion of the heated shock layer is more than the ratio of 9 to 1, the heating requirement of the gas mixture can be lowered

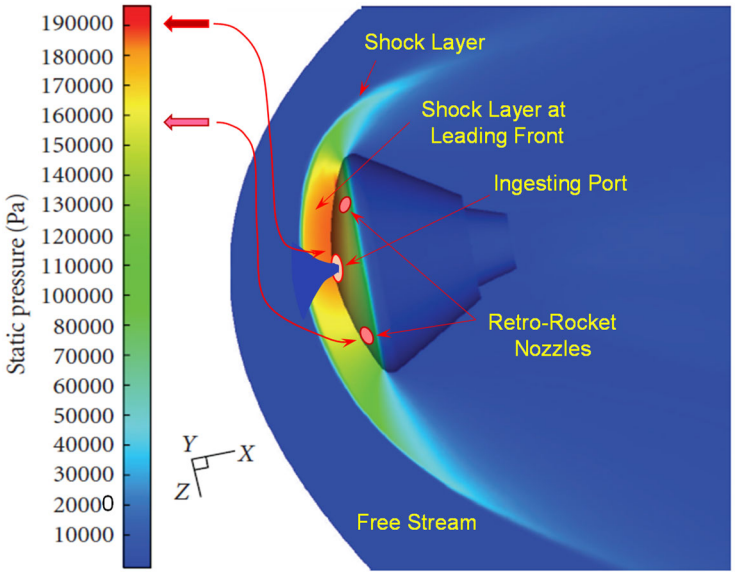

Figure 6. Static pressure at stagnation & downstream (under the courtesy of publisher [17])

further. The heated gas mixture is directed through the retropropulsion tubes where the heated gas is expanded and ejected through nozzles located at the downstream of shock layer to gain retropropulsion (see Figure 3 and Figure 4). The static pressure of downstream is much lower than the total pressure at the entrance of the ingesting port. This difference in pressure is an additional advantage for expanding and driving the heated gas flow through the nozzles. Heating the gas mixture requires a compact and high-density power system that will fit into the limited space within the entry vehicle.

Since the trajectory of an entry vehicle is determined by the entry insertion angle and atmospheric density, the vehicle must monitor its entry speed for the next stage of operation. The Martian atmospheric data given by Susaria, R. et al. [13] are from measurements done with the flights of Viking, MER Spirit, MER Opportunity, and Pathfinder. Specifically, the measured density vs. altitude data in the Martian atmosphere by the Pathfinder, Viking Upper Atmospheric Mass Spectrometer (VUAMS) and Viking Atmospheric Structure Instrument (VASI) probes were compared with the result of analytical model of Drake, D. et al. [14]. The theoretical results were very close to the measured density data. The measured density data by VUAMS and VASI probes were used for this analysis.

The dynamics of the entry vehicles are varied not only by the insertion angle and the density of the rarefied Martian thermosphere, but also by the angle of attack (AoA) of the vehicles through the Martian atmosphere. The pressure variance by the AoA was studied by Prezzella, G. and Viviani, A. [17] (see Figures 18 and 19 of Ref. 17). The pressure ratios of the gases over the leading head of the vehicle were different for the cases of 0-degree AoA (normal) and 10-degree AoA (oblique) [17]. In an oblique entry (10-degree AoA), the pressure ratio between the wall (P_w) and free-stream (P_{t2}) was 0.7 at the point ($s/R_b = -0.8$) from stagnation center line, as compared to 0.8 at the point ($s/R_b = -0.8$). The pressure downstream ($s/R_b = -0.8$) in the oblique entry was 10% lower than in the normal entry. In both cases, the down-stream pressures were 20% lower for normal entry and 30% lower for oblique entry, respectively, as compared to the stagnation point. This pressure difference between the stagnation and the downstream points can be interpreted favorably into these new applications where the ingested gas flows through the port at the leading head and splits among heating chambers and expands through thrust nozzles circumferentially located at sidewall ($\boldsymbol{P_W}$) where the downstream condition is set at $\boldsymbol{s/R_b}$ = - 0.8.

III. Analysis Approach and Results

III-1. Basis for Calculations

All the parameters discussed in Section II were used to estimate the thrust for retropropulsion and specific impulse (Isp). As tabulated in Table 2 and Table 3, the variables include the data from Table 1 using the same altitude points that are regarded as the flight corridor for supersonic retropropulsion operation. The baseline approach for estimation is to use the temperature of the mixed stream between the shock layer and freestream. The parameters to calculate the mixture temperature and the energy needed to raise the mixture temperature to 2800 K were collected from various research results cited in Section II. The range of retropropulsion operation is from

100 km down to 10 km as marked on Figure 2 with the entry vehicle velocity taken from the entry data of the MER Spirit and MER Opportunity Landers [14]. The temperature in Celsius, the pressure in kPa, and the front shock density in kg/m^3 were taken from the calculations shown in Table 1 that were made from the formula given by NASA Glenn Research Center (GRC) [15] on upper atmospheric calculations. Density jump-off (JO) data was obtained from the study results on density versus altitude by Drake, J.R. et al. [14].

The shock layer density can be calculated (see Equation 1) using the density ratio of free-stream and shock-layer from the jump-off data given by Leibowitz, M.G. and Austin, J.M. [9]

$$\boldsymbol{\rho_{SL} = 10 \cdot \rho_{FS}} \qquad (\mathbf{1})$$

where $\boldsymbol{\rho_{SL}}$ is the density at shock-layer and $\boldsymbol{\rho_{FS}}$ the density of free-stream.

By considering that approximately 10% of the shock layer (that formed around the port opening in the forebody) falls into the port opening and mixes with the incoming free-stream, a density of the gas mixture in the inlet is estimated (see Equation 2)

$$\boldsymbol{\rho_{inlet} = 0.9 \cdot \rho_{FS} + 0.1 \cdot \rho_{SL}} \qquad (\mathbf{2})$$

The flowrate of the ingested gas mixture is determined as a vital element in propulsion systems. The speed of the gas mixture that travels through the system determines the flowrate. The flowrate (see Equation 3) is defined by the multiplication of the entry vehicle velocity obtained from the entry data of the MER Spirit and MER Opportunity Landers [14], the density at the inlet calculated from Equation 2, and the constant inlet area, which is set for this study as 0.2826 m^2.

$$\boldsymbol{\dot{m} = V_{vehicle} \cdot \rho_{inlet} \cdot \dot{A}_{inlet}} \qquad (\mathbf{3})$$

Table 2. Performance estimation of new retropropulsion with NTAC power.

Altitude, km	Vehicle Velocity, m/s	Density FS, kg/m^3	Density SL, kg/m^3	Density, JO, kg/m^3	Density, Inlet, kg/m^3	Inlet Area, m^2	Flowrate, kg/s
100	5600	0.0000162	0.000162	0.0000005	0.00003078	0.2826	0.049
80	5500	0.0000376	0.000376	0.000002	0.00007144	0.2826	0.111
60	5400	0.0001411	0.001411	0.0003	0.00026809	0.2826	0.409
50	5300	0.0002914	0.002914	0.0008	0.00055366	0.2826	0.829
40	4400	0.0006179	0.006179	0.001	0.00117401	0.2826	1.460
30	3000	0.0013356	0.013356	0.004	0.00253764	0.2826	2.151
20	1500	0.0029298	0.029298	0.01	0.00556662	0.2826	2.360
10	450	0.0065028	0.065028	0.04	0.01235532	0.2826	1.571

Altitude, km	Temperature K	Pressure, kPa	Density, FS kg/m^3	P_{bs} kg.m/s^{2}m^2	$V_{delta\ P}$ m/s	Density, SL kg/m^3	Density, comb kg/m^3
100	27.76	0.00008625	0.0000162	0.08625	5599	0.000162	0.00005994
80	72.15	0.00052186	0.0000376	0.52186	5499	0.000376	0.00013912
60	116.55	0.0031571	0.0001411	3.1571	5398	0.001411	0.00052207
50	138.75	0.00776521	0.0002914	7.76521	5297	0.002914	0.00107818
40	160.75	0.01909933	0.0006179	19.09933	4396	0.006179	0.00228623
30	183.15	0.04697674	0.0013356	46.97674	2994	0.013356	0.00494172
20	205.35	0.11554406	0.0029298	115.54406	1486	0.029298	0.01084026
10	227.55	0.28419219	0.0065028	284.19219	399	0.065028	0.02406036

The temperature of the shock layer near the stagnation region of the forebody was found from the data of the MER Opportunity [14]. For this study, using 10% of the shock layer temperature and adding it with 90% of the ambient temperature, the temperature of the resulting gas mixture is estimated by the following ratio (see Equation 4)

$$T_{mixed} = 0.9 \cdot T_{ambient} + 0.1 \cdot T_{shock} \qquad (4)$$

The power for heating the mixture was calculated (see Equation 5) using the specific heat of CO_2, 1.397 kJ/kgK, multiplied by the flowrate in kg/s calculated from Equation 3 which is then multiplied by the maximum temperature of 2800 K minus the mixed temperature in kelvin calculated from Equation 4. The increase in gas pressure by heating the ingested gas up to 2800 K is estimated by Equation 5 as

$$P_{Heating} = 1.397 \cdot \dot{m} \cdot (2800 - T_{mixed}) \qquad (5)$$

The entry pressure for the vehicle was calculated (see Equation 6) using the vehicle velocity in m/s multiplied by the flowrate in kg/s, and then divided by the inlet area of 0.2826 m^2.

$$p_{enter} = \frac{V_{vehicle} \cdot \dot{m}}{A_{inlet}} \qquad (6)$$

After mixing in the passage, the gas mixture is heated to the maximum allowed temperature, 2800 K, by a heating element located inside the flow channel. This pressure of heated gas is estimated (see Equation 7) by multiplying the gas constant with the maximum temperature of 2800 K and the flowrate calculated by Equation 3 and dividing by the inlet area,

$$p_{Heating} = \dot{m} \cdot R \cdot \frac{2800}{A_{Inlet}} \qquad (7)$$

The exit velocity of heated gas was calculated using Equation 8 as follows:

$$V_{Heating} = \sqrt{\frac{2\gamma}{\gamma - 1}\frac{RT_{max}}{M}\left[1 - \left(\frac{p_{exit}}{p_{inlet}}\right)^{(\gamma-1)/\gamma}\right]} \qquad (8)$$

The specific Impulse was calculated (see Equation 9) by dividing Equation 8 by the gravity constant (9.81) .

$$Isp = \frac{V_{Heating}}{9.81} \qquad (9)$$

The original thrust was calculated (using Equation 10) by the flowrate from Equation 3 multiplied by $V_{heating}$ from Equation 8.

$$Thrust = \dot{m} \cdot V_{Heating} \qquad (10)$$

For the pressure behind the shock layer, the pressure value was selected from Table 1 and multiplied by 1000 for pascal (kPa→ $kg \cdot m^{-1} \cdot s^{-2}$) to convert to like units.

The flow velocity created by the pressure difference was calculated (see Equation 11) using the entry pressure from Equation 6 minus the pressure behind the shock which is then multiplied by the Inlet Area and divided by the flowrate from Equation 3.

$$V_{\Delta P} = (p_{Enter} - p_{BS}) \cdot \frac{A_{Inlet}}{\dot{m}} \qquad (11)$$

The exit velocity was calculated by combining $V_{Delta\text{-}p}$ and V_{Heat}

$$V_{Exit} = V_{\Delta p} + V_{Heating} \qquad (12)$$

$Isp_{\Delta p}$ was calculated by the velocity $V_{\Delta p}$ divided by acceleration constant of 9.8

$$Isp_{\Delta p} = \frac{V_{\Delta p}}{9.8} \qquad (13)$$

$Thrust_{delta\text{-}p}$ was calculated by flowrate from Equation 3 multiplied by $V_{\Delta p}$

$$Thrust_{\Delta p} = \dot{m} \cdot V_{\Delta p} \qquad (14)$$

Isp_{Total} was calculated by exit velocity divided by acceleration constant. It can also be added up with Isp and $Isp_{\Delta p}$.

Table 3. Performance estimation of new retropropulsion with NTAC power.

Ambient Temp, K	Shock Temp, K	Mixed Temp, K	Heating Power, kW	P_{enter} kgm/m^2	$P_{heat,}$ kgm/m^2	V_{heat} m/s	Isp s	Thrust N
300.86	18200	2091	48	965	91.18	2159	220	105
345.25	18200	2131	104	2161	207.85	2157	220	239
389.65	18100	2161	365	7818	765.79	2155	220	882
411.85	17000	2071	845	15552	1552.23	2155	220	1787
434.05	13000	1691	2262	22729	2732.50	2153	220	3144
456.25	5500	961	5528	22839	4027.05	2151	220	4629
478.45	2500	681	6987	12525	4416.91	2148	219	5068
500.65	1200	571	4894	2502	2941.05	2140	218	3363

V_{exit} m/s	Isp_{Total} s	$Thrust_{Total}$ N	$Isp_{delta\ P}$ s	$Thrust_{delta\ P}$ N	Power MW	Power W	Thrust Gain %	
							Av Gain	41%
7759	792	378	571	273	0.05	48263	28	
7655	781	850	561	611	0.10	103819	28	
7553	771	3090	551	2208	0.37	365391	29	
7452	760	6180	541	4393	0.84	844918	29	
6550	668	9561	449	6418	2.26	2262370	33	
5145	525	11070	305	6441	5.53	5528281	42	
3634	371	8575	152	3507	6.99	6986559	59	
2539	259	3990	41	627	4.89	4893572	84	

$$Isp_{Total} = \frac{V_{Exit}}{9.8} \qquad (15)$$

$Thrust_{Total}$ was calculated by flowrate multiplied by the exit velocity (at the nozzle)

$$Thrust_{Total} = \dot{m} \cdot V_{Exit} \qquad (16)$$

The power needed in MW was calculated by heating power (in kW) divided by 1000

$$P_{MW} = \frac{P_{Heating}}{1000} \qquad (17)$$

III-2. Performance Analysis of new retropropulsion system

The graphs in Figure 7 through Figure 12 were made using the variables calculated from the formulas and data and charts obtained from the references. The velocity of entry vehicle along

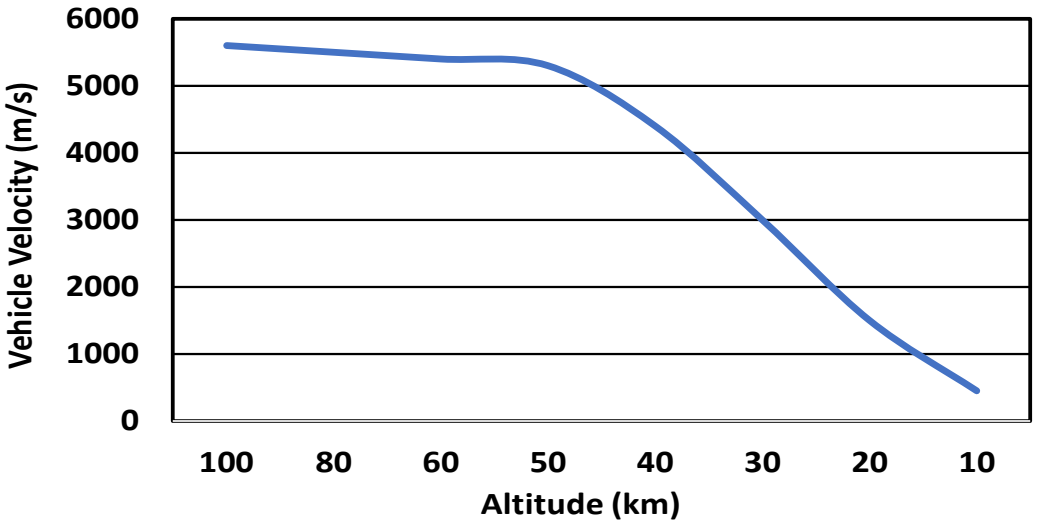

Figure 7. Vehicle Velocity with aerodynamic braking in Mars entry process (estimated from reference 14)

the entry trajectory under the aerodynamic braking through the flight corridor with respect to altitude (see the second column of Table 2 from Ref. [14]) is shown in Figure 7. The entry velocity profile shown in Figure 7 is an estimated result based on the velocity profile of the MER Spirit and MER Opportunity Landers [14] by accounting for aerobraking to eventually reduce vehicle entry velocity down to 450 m/s level so that parachutes can be safely deployed at the altitude of 10 km. The velocity profile shown in Figure 7 is the pattern that this new retrorocket concept needs to follow by reducing the vehicle velocity using the heated thermal expansion of ingested propellant flow attributed to the pressure difference between the stagnation pressure at the leading front and the static pressure downstream where the retropropulsion nozzles are located as shown in Figure 3, Figure 4, and Figure 6. This velocity profile is also dependent on the density profile of the Martian atmosphere [14, 18].

Shown in Figure 8 are the nozzle exit velocities of ingested gas for the flow caused by the pressure difference between the stagnation and downstream (orange colored line), the flow by the expansion of thermally heated gas (blue colored line), and the flow combined with both flows by pressure difference and thermal expansion (grey colored line). The flow caused by the pressure difference between the stagnation and downstream points is substantially high as shown in Figure 7. Since the stagnation pressure is substantially high as compared to the pressure downstream, the ingested gas flows through each split heating channel with a fast velocity. For the flow caused by the expansion of thermally heated gas, a net amount of ingested gas is heated to the maximum

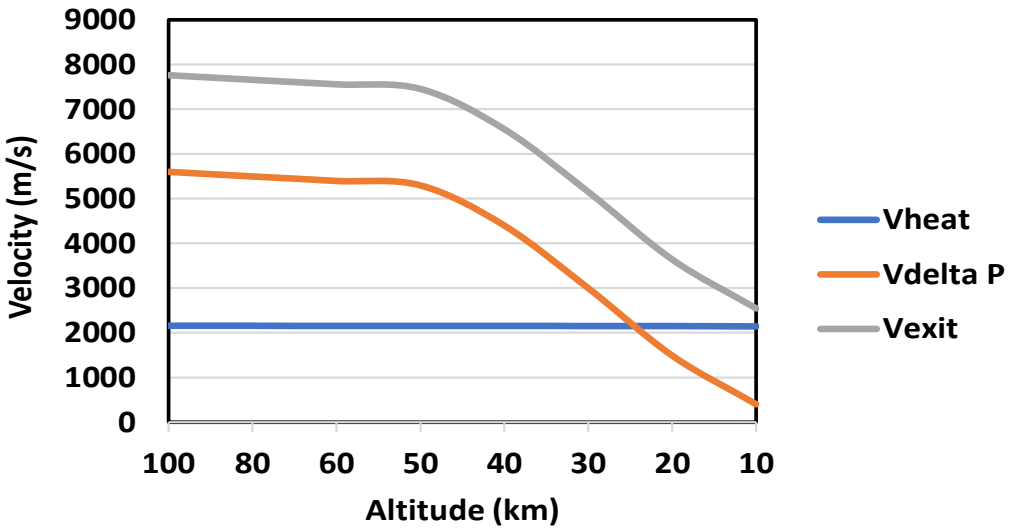

Figure 8. Nozzle exit velocities for the flow caused by the pressure difference between stagnation and downstream points (orange line, Eq. 11), the expansion of heated gas up to 2800 K (blue line, Eq. 8), and the combined (grey line, Eq. 12).

allowable temperature, 2800 K. No matter how much gas is ingested along the entry corridor, the ingested amount of gas is constantly heated to 2800 K. In retropropulsion, the portion of heated flow is added up to increase the overall exit velocity through nozzle. Shown in Figure 9 are the specific impulses defined with the velocities of nozzle exit flows identified in Figure 8. At the altitude of 25 km where the flow speed of ingested gas slows down along with aerodynamic braking, the flow speed by the expansion of heated gas surpasses the flow speed run by the pressure difference. When the entry vehicle descends, the velocity decreases with the increase in density. Accordingly, the stagnation pressure at the leading front is reduced too. In this case, the velocity caused by the pressure difference between the stagnation and downstream point, where the retropropulsion nozzles are located, is reduced. That is why the contribution of the pressure difference to the nozzle exit velocity is lower as compared to that of the heated gas around 25 km altitude. Plotted in Figure 9 are the specific impulses for the flows described by the flows in Figure 8. Illustrated in Figure 10 are the thrusts of retropropulsion system based on the nozzle exit velocities as defined in Figure 8. In Figure 10, a substantial thrust gain by heating the ingested gas (blue line) contributes to the decrease in velocity of the entry vehicle. The thrust gain alone (blue line in Figure 10 and see the last column of Table 3) by the power injection from the

NTAC system comprises of approximately 41 % of the total thrust required for retropropulsion. On the other hand, it can be linearly interpreted as the 41% saving of propellant if propellant for

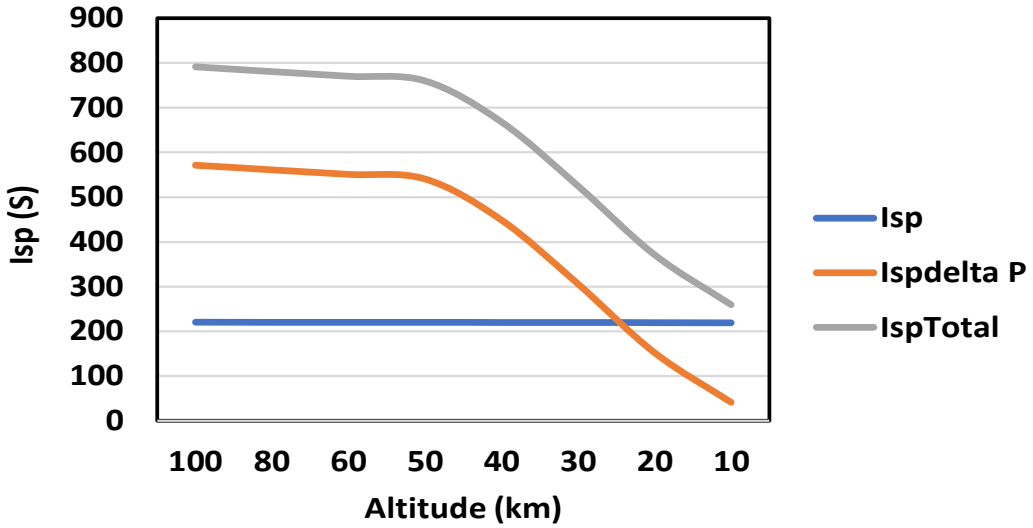

Figure 9. Specific impulses, Isp, of retropropulsion thruster for the flows by pressure difference (orange line, Eq. 13) and expansion of thermally heated gas (blue line, Eq. 9), and Total Isp (grey line, Eq. 15).

retropropulsion is used or as the 41% more aerodynamic drag that might tolerate steeper angle entry or as much more reduced entry velocity at 10 km altitude before deploying supersonic

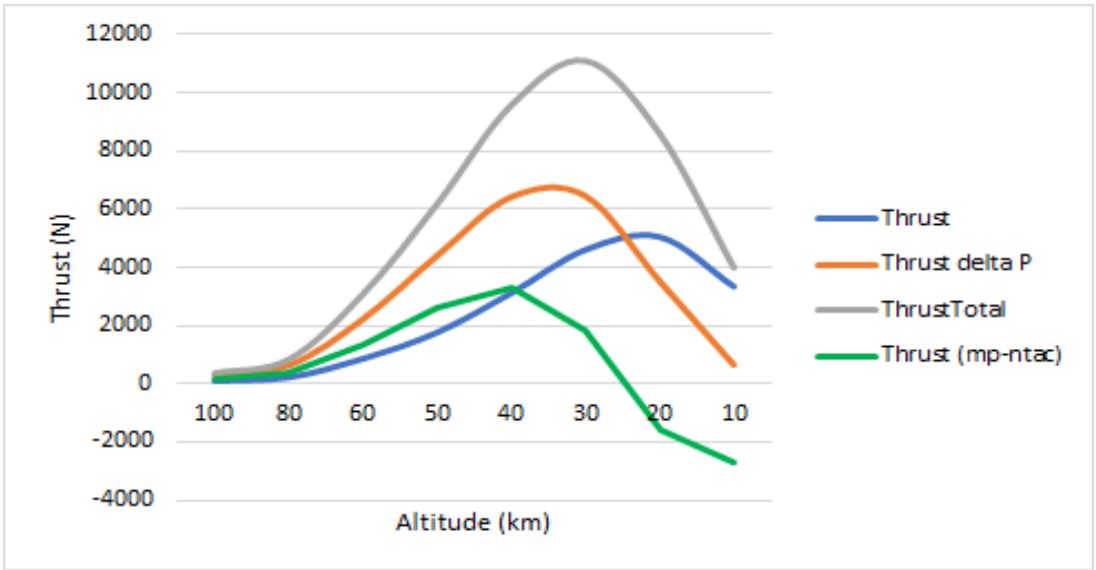

Figure 10. Thrust obtained by heating ingested gas (blue line, Eq. 10), thrust obtained by operating thrusters as usual without NTAC on (orange line, Eq. 14), option for reduced thrust required by propellant thrusters with NTAC on (green line), thrust when both propellant thruster and NTAC retropropulsion are fully on (gray line, Eq. 16).

parachutes. More importantly, this additional thrust may be beneficial when landing larger payloads rather than to simply reduce the amount of propellant brought from Earth.

Suppose that a similar type of NTAC-assisted propulsion is applied for the launching mode to gain more thrust by heating the propellant gas, especially from the lunar or Mars base where NTAC operation is allowable. In such a launching mode, it is possible that the NTAC-assisted propulsion would save 10% to 20% of onboard propellant by the NTAC-assisted thrust gain.

Shown in Figure 11 is the power requirement to sustain the thrust gain by heating the ingested gas as a propellant. The retropropulsion system uses the power based on the altitude of the vehicle. While lowering the altitude of entry vehicle, the density of the Martian atmosphere keeps increasing and requires more power to heat it up to maintain the ingested gas at the maximum temperature, 2800 K. The power needed for the entry vehicle comes from the NTAC power system of which the specific power is very high and kept at the lowest system alpha as shown in Table 4. Based on the maximum power, 7.8 MW, required for retropropulsion through 20 km altitude in flight corridor as plotted in Figure 11, a 7-MW rated NTAC system listed in Table 4 is selected. A 7-MW rated NTAC system has the system α = 0.40 with the total weight of 3.045 metric tons. The dimensions of the 7-MW NTAC system is 1.684 m in diameter and 0.259 m in height. The actual power output of a 7-MW rated NTAC system is 8.607 MW which is 23% more than the rated and suffices the power needs for this new retropropulsion system concept.

After successful landing of the Mars probe, the NTAC system can be separated from the retropropulsion system, if necessary, as described by the dotted line in Figure 3. Then it can be used as a surface power source for Martian exploration since NTAC runs several years without refueling.

The specifications of the NTAC systems based on the specific amount of power from 1 megawatt to 15 megawatts level is shown in Table 4. If Mars exploration requires a surface power for

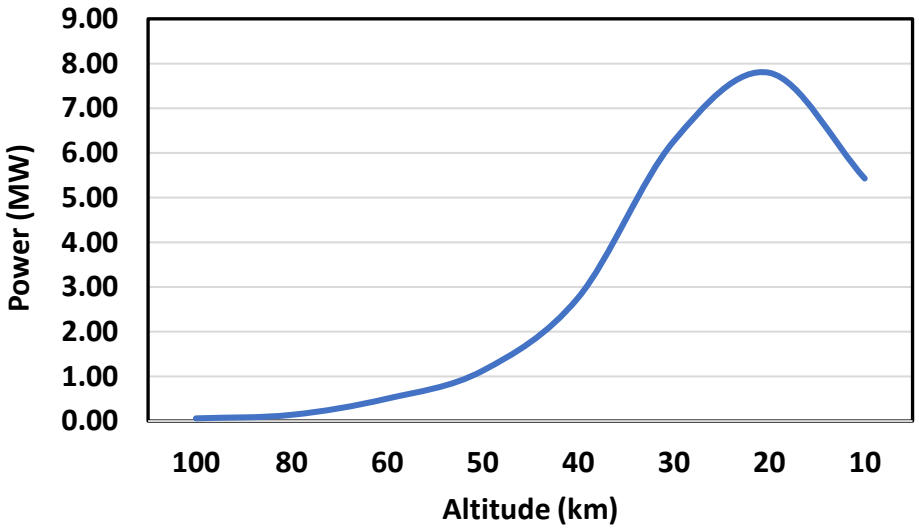

Figure 11. Power required to slow down entry vehicle (Eq. 17).

Table 4. Performance of NTAC power system for new retropropulsion system [8]

Power Rating, MW	Power Output, MW	NTAC Output, MW	MJ-TE Output, MW	NTAC Weight, kg	Shielding Weight, kg	MJ-TE Weight, kg	Total Weight, kg	Diameter (D), m Height (H), m	NTAC Specific Power, kW/kg	NTAC System α, kg/kW
1	1.858	1.567	0.291	307	273	217	1050	D: 1.084 H: 0.229	1.587	0.630
2	2.549	2.150	0.399	369	321	254	1292	D: 1.184 H: 0.234	1.754	0.570
3	3.085	2.602	0.483	447	382	301	1763	D: 1.284 H: 0.259	2.325	0.430
4	5.507	4.645	0.862	518	437	343	2050	D: 1.384 H: 0.259	2.381	0.420
5	6.464	5.452	1.012	595	495	388	2360	D: 1.484 H: 0.259	2.439	0.410
6	7.497	6.323	1.174	676	557	435	2691	D: 1.584 H: 0.259	2.500	0.400
7	**8.607**	**7.259**	**1.348**	**763**	**622**	**485**	**3045**	**D: 1.684 H: 0.259**	**2.500**	**0.400**
8	9.792	8.259	1.533	743	704	547	3420	D: 1.784 H: 0.259	2.564	0.390
10	12.529	10.567	1.962	960	770	598	4038	D: 1.884 H: 0.269	2.778	0.360
15	16.525	13.937	2.588	1076	857	664	4852	D: 1.984 H: 0.284	3.448	0.290

specific exploration missions, then the NTAC system can be the best candidate power system that can be used for both retropropulsion of Mars entry probes and surface power. Based on previous analysis, NTAC seems capable of supplying megawatt level power within the maximum allowable volume and weight of an entry vehicle. Hence, the NTAC power system seems compatible for the EDL applications since it is a compact and long-lasting high performing power system with very high specific power (> 1 kW/kg) [8].

IV. Conclusion

The new concept studied here for the retropropulsion system for Mars entry probes and landers is very attractive since the retropropulsion system can use the Martian air as propellant. By ingesting the Martian air through a port built in the middle of stagnation region, it can avoid a thermally loaded hot spot building on the leading-edge area of vehicle by the radiation from the shock. Multi-channel thrust nozzles can evenly distribute retrorocket thrust of vehicle. The flowrate of ingested gas can be flexibly distributed to control the vehicle operation. Heating rate control on each CO_2 propellant channel separately is possible by power modulation which will offer the maneuverability of Mars entry vehicles. The estimation shows that the thrust gain by heating the ingested gas as propellant is substantial for retropropulsion. Further study is required to quantify the effect of added mass vs. the increase in thrust enabled by NTAC to identify infusion of this technology for landing larger payloads on Mars. The previous EDL procedure had the propulsion system fly off once the rover safely landed. The NTAC system can be a surface power source for a variety of Mars exploration missions after the retropropulsion role is over.

A similar application of NTAC can be extended to the thruster of initial launching vehicle for additional thrust gain by heating the propellant gas in combustion chamber. Such an application of NTAC may require whole new analyses in terms of configuration, integration, and operation of new propulsion system to quantify the specific benefits of NTAC. Accordingly, the added mass of NTAC to the payload that provides the increase in thrust for initial launching is not included in this study.

References

[1] NASA Science, Mars Exploration Program, “Historical log of Mars Missions,” https://mars.nasa.gov/mars-exploration/missions/historical-log/, August 5, 2022.

[2] Perminov, V.G., “The Difficult Road to Mars, Monographs in Aerospace History,” No. 15, July 1999.

[3] Shapland, D.J., Price, D.A., and Hearne, L.F., “A Configuration for Re-Entry from Mars Missions Using Aerobraking,” J. Spacecraft, Vol. 2, No. 4, July-Aug. 1965

[4] https://mars.nasa.gov/odyssey/mission/timeline/mtaerobraking/, August 5, 2022.

[5] Lu, Y., “Aerocapture, Aerobraking, and Entry for Robotic and Human Mars Missions,” a chapter in *Mars Exploration*, edited by Pezzella, G. and Viviani, A., Aug. 4, 2020

[6] NASA/JPL-Caltech, https://mars.nasa.gov/mars2020/timeline/landing/entry-descent-landing/ August 7, 2022.

[7] Korzun, A.M., Cruz, J.R., and Braun, R.D., “A Suvey of Supersonic Retropropulsion Technology for Mars Entry, Descent, and Landing,” 2008 IEEE Aerospace Conference, 01-08 March 2008, Big Sky, MT, DOI: 10.1109/AERO.2008.4526290

[8] U.S. Patent No. 10,269,463, “Nuclear Thermionic Avalanche Cells with Thermoelectric (NTAC-TE) Generator in Tandem Mode,” April 23, 2019

[9] Leibowitz, M.G. and Austin, J.M., “Hypervelocity Spherically-Blunted Cone Flows in Mars Entry Ground Testing,” AIAA J. Vol. 59, No. 9, Sep. 2021

[10] The Planetary Atmospheres Node, NASA Planetary Data System, https://pds-atmospheres.nmsu.edu/data_and_services/atmospheres_data/MARS/mars_lander.html

[11] Smith, M.D., “Spacecraft Observations of the Martian Atmosphere,” Annual Review of Earth and Planetary Sciences, Vol. 36, pp.191-219, 2008

[12] Withers, P. and Catling, D.C., “Observations of Atmospheric Tides on Mars at the Season and Latitude of the Phoenix Atmospheric Entry,” Geophysical Research Letters, Vol. 37, No. 24, L24204, 2010

[13] Susaria, R., Jain, S.K., and Bhardwaj, A., “Forbidden Atomic Oxygen Emissions in the Martian Dayside Upper Atmosphere,”, https://www.researchgate.net/publication/346933661_Forbidden_atomic_oxygen_emissions_in_the_Martian_dayside_upper_atmosphere, August 5, 2022.

[14] Drake, D.J, Popovic, S., Vuskovic, L. and Dinh, T., “Kinetic Description of Martian Atmospheric Entry Plasma,” IEEE Transactions on Plasma Science 37(8):1646 – 1655, Sept. 2009

[15] https://www.grc.nasa.gov/www/k-12/airplane/atmosmrm.html, July 17, 2022.

[16] The Engineering ToolBox: U.S. Standard Atmosphere Air Properties vs. Altitude - SI Units, https://www.engineeringtoolbox.com/standard-atmosphere-d_604.html, July 17, 2022.

[17] Pezzella, G. and Viviani, A. “Aerodynamic Analysis of a Manned Space Vehicle for Missions to Mars,” *Journal of Thermodynamics*, Vol. 2011, ID 857061, doi:10.1155/2011/857061

[18] Forget, F., et al. “Density and Temperatures of the Upper Martian Atmosphere Measured by Stellar Occultations with Mars Express SPICAM,” Journal of Geophysical Research, Vol. 114, E01004, Doi:10.1029/2008je003086, 2009.